WAKE FIELD MONITORS IN A MULTI PURPOSE X BAND ACCELERATING STRUCTURE

M. Dehler, S. Bettoni, B. Beutner, PSI, Villigen PSI, Switzerland
G. de Michele*, PSI, Villigen, EPFL, Lausanne and CERN, Geneva, Switzerland

Abstract

In a collaboration between CERN, PSI and Sincrotrone Trieste (ST), a series of four multipurpose X-band accelerating structures has been designed and fabricated. These feature integrated wake field monitors (WFMs), which are used to measure the alignment (offset and tilt) between structure and beam. One structure has recently been installed in the SwissFEL Injector Test facility (SITF) at PSI. The WFM front end electronics will be developed within the EuCard2 framework, so for the measurements described in this paper we used the raw WFM signals. We compare these measurements to the theoretical results obtained via an equivalent circuit model used in the design and numerical calculations. The beam tests show that by minimizing the WFM signals, the emittance dilution given by the transverse wakes, crucial because of the small aperture of the structure, is minimized as well.

INTRODUCTION

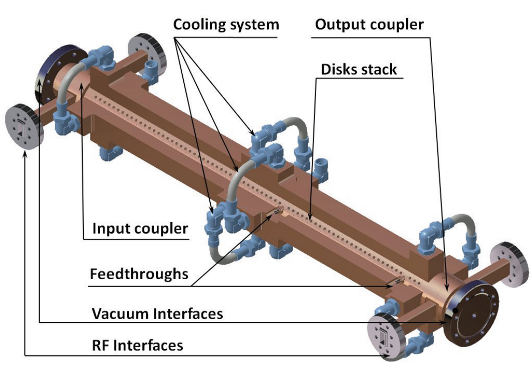

Figure 1: General view of accelerating structure.

A series of multipurpose X band structures (Fig. 1) at the European frequency of 11.99 GHz has been developed and built in collaboration between CERN, PSI and ELETTRA. At PSI and ELETTRA, it will serve for longitudinal phase space compensation at the respective FEL projects (Fig. 2 shows an example for SITF, for ELETTRA see [1]). CERN will use one of the produced structures to test break down limits and rates in the high gradient regime.

The design employs a large iris, $5\pi/6$ phase advance geometry, which minimizes transverse wake field effects while still retaining a good efficiency. The basic specifications are given in Table 1, more information for the design can be found in [2, 3] and for the fabrication in [4, 5, 6]. Beam degradation due to transverse single bunch wake fields are a concern for the application for free electron laser: Two wake field monitors, providing signals from the dipole modes inside the structure, have been integrated to monitor the beam to structure alignment with a resolution better than 10 μm.

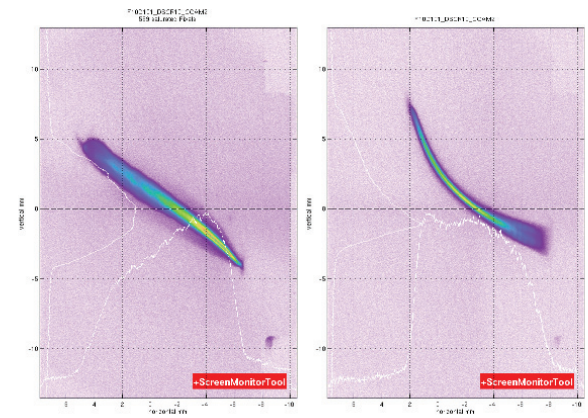

Figure 2: Correction of longitudinal phase space nonlinearity using the X band structure: Charge distribution at the end of SITF streaked with an RF deflector, horizontal axis corresponds to longitudinal coordinate inside the bunch. Left with X band structure, right without.

Table 1: Specifications

Beam Voltage	30 MeV
Max. Power	29 MW
Frequency (40° C)	11.991648 GHz
Iris diameter	9.1 mm (avg.)
Wake field monitors	up/downstream
Operating temp.	40° C
Fill time	100 ns
Repetition rate	100 Hz
Structure length	965 mm

Wake Field Monitors

One of the characteristics of a constant gradient structure is the smooth variation of the cell dimensions along the structure, which compensates for internal losses and keeps the gradient of the fundamental mode constant. This leads to a spread of the synchronous frequency of the position dependent dipole modes. Upstream, an offset beam will excite lower dipole mode frequencies than downstream. Also,

* he would like to thanks A. Grudiev for suggestions and discussions on GdfidL EM simulation

ISBN 978-3-95450-127-4

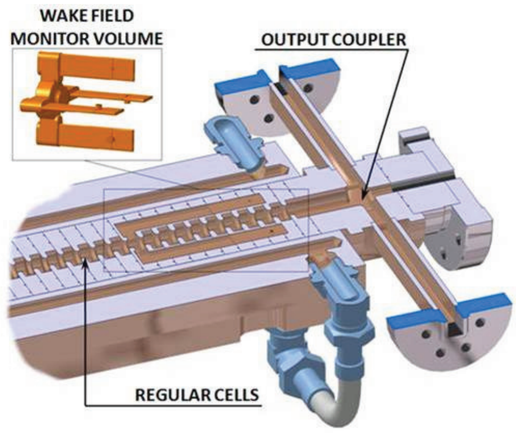

Figure 3: Wake field monitors geometry.

the modes will not extend throughout the structure, but will be confined. To capture as much information as possible, two sets of monitors were used, one sitting in the middle coupling to dipole modes in the upstream half of the structure and another towards the downstream end for the other part.

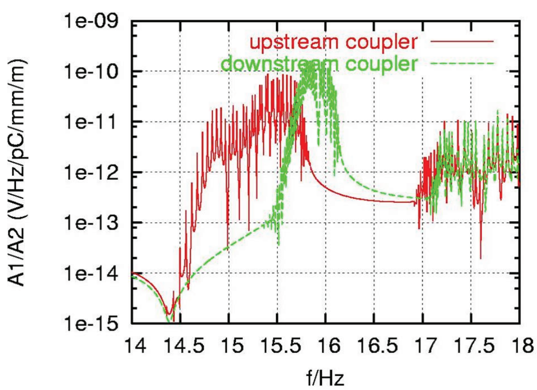

Figure 4: Theoretical signal spectrum.

As the signals of interests are in the sub milliwatt range, while the fundamental mode is powered with tens of megawatts, an important criterion in the design of the WFM is to eliminate any coupling of the fundamental mode into the monitor output. Furthermore we would like to see a purely position dependent signal, meaning that there should be no trace of higher order longitudinal modes. This was achieved by the coupling geometry shown in figure 3, a hollow waveguide is coupled to the coupling cavity so, that it rejects any longitudinal modes by symmetry. The chosen cutoff frequency further attenuates any trace of the fundamental 12 GHz before transitioning into a coaxial feedthrough. Figure 4 shows the theoretical spectrum [2, 7]. It should be mentioned, that higher order misalignments show up as distinctive patterns in the spectrum, something we show practically in the next section.

A WFM is comparable to a classical cavity BPM in that we have position dependent signals, but there is an important difference. We are having signals which are directly proportional to the wakes and so to the degradation of the beam and the golden orbit with respect to the structure is given by minimum amplitudes, whereas a BPM needs a secondary procedure like e.g. based alignment alignment to get this reference. This acts also as a self diagnostic tool: elevated amplitudes at the minimum indicate problems with the internal alignment.

RESULTS WITH BEAM

In the absence of a dedicated RF front end (which will be developed in the next years as part of the EuCARD2 project [8]), we restricted ourselves to the measurement of raw signals. The wake field monitors were connected to a fast real time scope outside the tunnel via 8 meter long cables (Huber & Suhner Sucoform 86). Most of the measurements were done using a LeCroy SDA816zi digital scope with 18 GHz bandwidth and 40 GS/s sample rate. To get a view of the wide bandwidth response, we were able to rent a LeCroy 9Zi-A scope with 45 GHz bandwidth and 120 GS/s.

As was mentioned before, the signal minimum gives also the minimum degradation of the beam due to transverse wakefields. Since there is a golden orbit given by the optimum beam trajectory through the focusing magnets, the accelerating structure is sitting on a mover system to align the structure to the beam. For best beam performance in terms of emittance, we used this system to measure the response versus the beam offset.

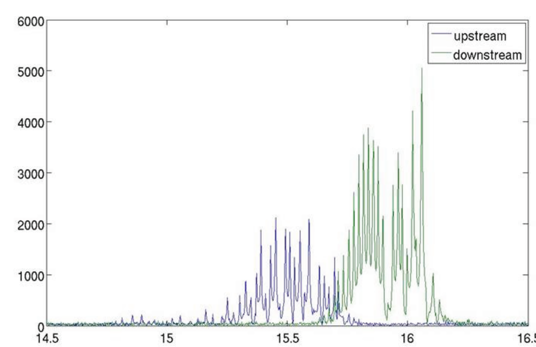

Figure 5: Measured signal spectrum.

Figure 5 shows the signal spectra of the up- and downstream monitors with an offset structure. The two complementary frequency spectra of the two monitors corresponding to the different parts of the structure match the theoretical results of figure 4 quite well, which have been computed with an equivalent circuit model. The signal distortion due to reflections at the cable transitions, which is clearly visible in the time domain, make is somewhat difficult to compare signal levels. But nonetheless the measured peak amplitudes of 10 V/nC/mm (corrected for the attenuation in the connecting cables) fit relatively well with the value of 6 V/nC/mm of the equivalent circuit model (which omits high order dipole bands) and 4 V/nC/mm calculated

ISBN 978-3-95450-127-4

with CST Particle Studio [9] (which, due to CPU time restrictions, had to use a relatively long bunch length in the simulation also affecting the result).

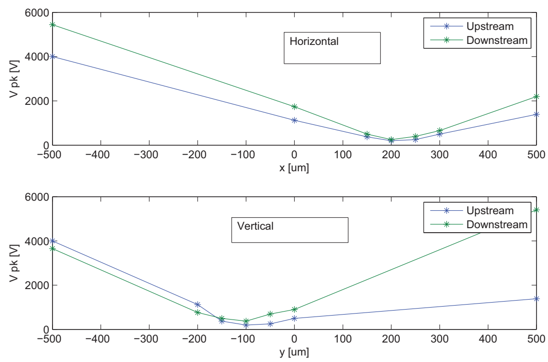

Figure 6: Signal amplitude versus beam offset.

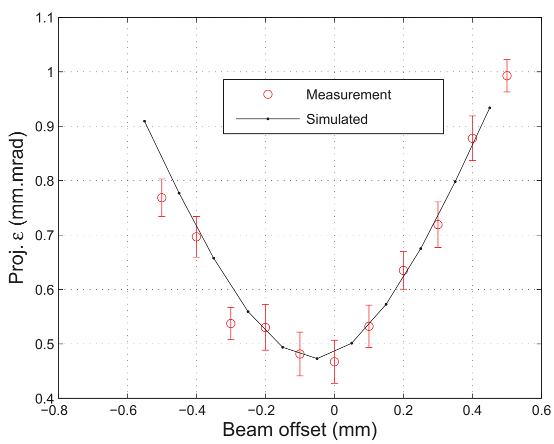

Figure 7: Emittance versus vertical offset.

The ultra fast scopes used for the measurement exhibit quite a bit of noise, which explains the relatively low resolution of the monitors as seen in figure 6. A dedicated front end, which is under development, should still give a strong improvement. Extremely interesting is to compare the optimum position given by the monitors with a measurement of the beam emittance versus beam offset. The monitors give the minimum at a vertical structure offset of -100 μm. Within the current resolution, the emittance measurement (Fig. 7) fits well with a result of -75 μm, proving the utility of this type of monitor.

To give an example of the measurement of a higher order misalignment, we tilted the structure (rotated around the vertical axis) and took the spectra. With a tilt, the center cells stay aligned to the beam, while the extreme parts of the structure see an offset. Given the correlation between frequency and position inside the structure, we expect a corresponding hole in the signal spectra as a typical pattern. Figure 8 confirms this quite clearly.

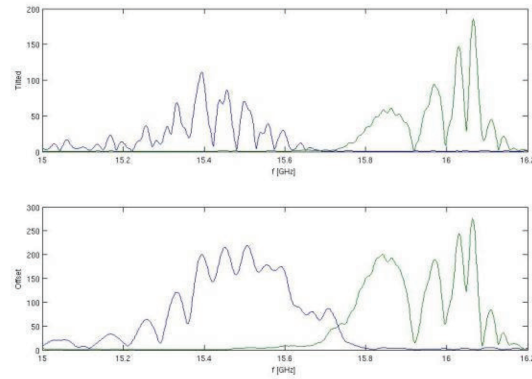

Figure 8: Comparison of signal spectra: structure tilt shows up as a characteristic hole in the spectrum as compared to an offset.

Higher Bands and Harmonics

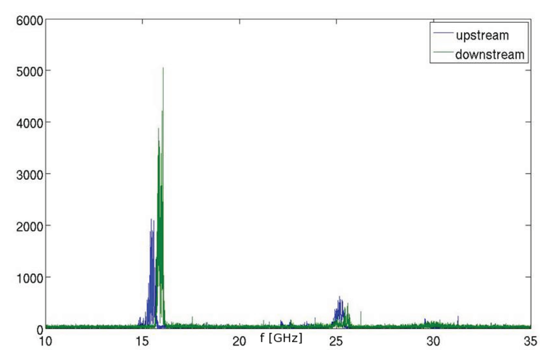

Figure 9: Wide band signal spectra.

The cables, connectors and feed throughs used were only specified up to 18 GHz, therefore the following results should only be interpreted qualitatively and not quantitatively.

Figure 9 shows the wide band responses of the monitors. For this measurement, there was no RF power in the structure. We see additional signals at 25 and 30 GHz. Aligning the structure to the beam minimizes also these spectral peaks, so that we can conclude them coming from higher order dipole bands, which was numerically verified by the simulations discussed in the next paragraph. No trace of a longitudinal, position independent mode was seen, which is an indication of an excellent internal mechanical alignment of the structure.

While the response for the lowest dipole bands can be compared to results using an equivalent circuit, the wide band response needed to be validated by a numerical calculation using GdfidL [10]. Both the complexity of the geometry and the large frequency bandwidth require a fine discretized structure, hence a necessity of parallel computing using up to 2 weeks of CPU time (the maximum time allowed at CERN). A grid resolution of 50μm is needed in terms of amplitude of spectra, the wake was calculated up to a length of 14m to give a reasonable frequency resolu-

ISBN 978-3-95450-127-4

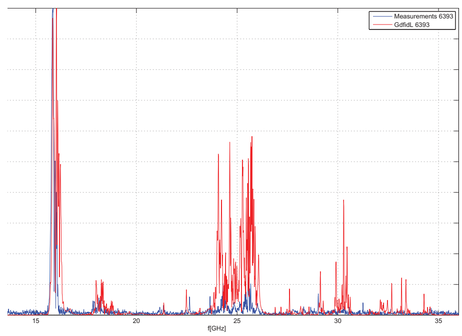

Figure 10: Wide band spectrum as calculated with GdFidl.

tion. Figure 10 shows the results for one of the downstream monitors. Up to 20 GHz, measurement and calculation correspond well. At higher frequencies, the amplitudes are not comparable due to the factors mentioned above, but none the less the dipole bands at 25 and 30 GHz are clearly visible.

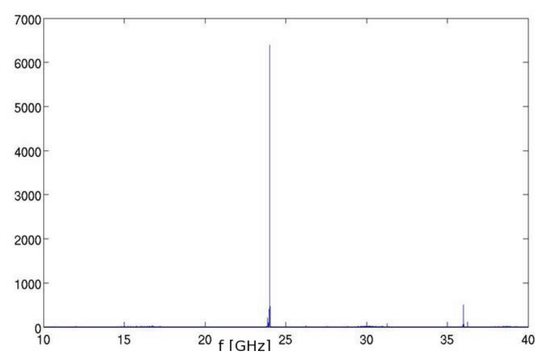

Figure 11: Harmonics of the X band klystron showing up in the WFM spectrum (no beam).

When switching on RF power in the order of 20 MW and without beam, there is no trace of the fundamental frequency (meaning a rejection of better than 120 dB), but we see spectral lines at the second and third harmonic of 24 and 36 GHz (Fig. 11). It is clear that nonlinearities in the klystron create harmonics, but normally we would expect them, due to symmetries in the waveguide network, to excite pure TM type modes in the structure (which, as was demonstrated with beam excitation, we don't see with the WFMs). For this reason, either mode conversion or symmetry errors in the network seem to be possible candidates creating that signal.

SUMMARY AND OUTLOOK

First tests with beam have been performed for our multi purpose X band structure, which features integrated wake field monitors giving informations about structure to beam alignment as offsets and tilts. We performed a characterization of the raw signals using ultra wide bandwidth scopes with the following results:

The signal levels and spectra correspond well to theoretical results obtained with numerical codes and equivalent circuit models. We were able to measure pure offsets as well as also higher order misalignments as tilts, which show up as a distinct pattern in the signal spectrum. An important result is the proof, that the monitors directly predict the optimum alignment position with respect to a minimum degradation of beam emittance.

A good indication of the precise internal assembly and alignment is the fact that we saw only position dependent signals in the wide band spectrum up to 45 GHz, neither the 12 GHz fundamental nor other longitudinal higher order modes were visible. Some leakage of the second and third klystron harmonic were visible - this will not cause problems for the operation of the monitor, but possibly for other wide band devices in the vicinity like e.g. a bunch arrival time monitor.

The measurements presented are limited in resolution by the noise in the very preliminary setup. Within the framework of EuCARD2 [8], we are currently in the process of starting the development of a dedicated front end, which should give us vastly better resolution. We would hope to reach theoretical resolution limit of a few μm determined by the mechanical precision of the structure assembly.

REFERENCES

[1] G. D'Auria et al. "RF Activation and Preliminary Beam Tests of the X-Band Linearizer at the FERMI@ELETTRA FEL Project", IPAC 2012, New Orleans, USA, TUPPP054 p. 1721 (2012)

[2] M. Dehler et al, "X-Band RF Structure with Integrated Alignment Monitors", Phys.Rev.ST Accel.Beams 12, 062001 (2009)

[3] D. Gudkov et al., "Engineering Design of a Multipurpose X Band Accelerating Structure", IPAC10, Kyoto, Japan, THPEA042, p. 3771 (2010)

[4] M. Dehler, et al., "Fabrication of the CERN/PSI/ST X-band Accelerating Structures", IPAC'11, San Sebastián, Spain, MOPC012, p86 (2011)

[5] J. Shi et al., "Tuning of CLIC Accelerating Structure Prototypes at CERN", LINAC2010, Tsukuba, Japan, MOP022, p. 97 (2010)

[6] M. Dehler et al. "A Multi Purpose X Band accelerating structure", IPAC 2012, New Orleans, USA, MOOBC003 p. 70 (2012)

[7] M. Dehler et al., "Numerical Validation of the CLIC/SwissFEL/FERMI Multi Purpose X Band Structure", LINAC2010, Tsukuba, Japan, MOP073, p. 223 (2010)

[8] http://eucard2.web.cern.ch/

[9] http://www.cst.de/

[10] http://www.gdfidl.de/

ISBN 978-3-95450-127-4